OSIRIS

Optical, Spectroscopic, and Infrared Remote Imaging System

Acquisition and processing of flat field images for OSIRIS calibration

RO-RIS-MPAE-TN-075

Issue: 2

Revision: -

20/12/2021

Prepared by:

Jakob Deller

Approval Sheet

Jakob Deller

Digitally signed by Jakob Deller
DN: cn=Jakob Deller, c=DE, o=Max Planck Institute for Solar System Research, email=deller@mps.mpg.de
Location: Goettingen
Date: 2021.12.20 15:08:54 +01'00'

prepared by: *Jakob Deller* (signature/date)

Digitally signed by Holger Sierks
Date: 2021.12.20 15:41:17 +01'00'

approved by: *Holger Sierks* (signature/date)

Document Change Record

Iss./Rev.	Date	Author	Pages affected	Description
Draft	5/5/2015	Tubiana, Da Deppo	all	First draft
1/-	6/7/2015	Tubiana, Da Deppo	all	First issue
1/a	23/11/2016	Tubiana, Da Deppo	Section 2.3, Section 2.4, Section 3	New section
1/b	22/2/2017	Tubiana	Section 4	Section added
2/-	20/12/2021	Deller	Table 4	Fixed UAX source reference for NAC filters 83, 84, 86 that where given as halogen but actually used xenon lamps.
			Section 2	Added description of normalization, increased version of corresponding files.
			Section 2.5	Added description and correction factors for facility artefacts removal for NAC flat-field images and updated list of flat field images used in the calibration pipeline.
			Section 3	Added Section
			Section 6	Updated version numbers of files used

Table of contents

List of Figures

List of Tables

1 General aspects

1.1 Scope

This document describes how the flat fields to calibrate OSIRIS images have been obtained. The description is based on the OSIRIS calibration report [RD5].

1.2 Reference Documents

no.	document name	document number, Iss./Rev.
RD1	Assessment of OSIRIS flat field data	RO-RIS-MPAE-TN-094
RD2	NAC and WAC Optical Band-pass Filter Transmissions	FILTER_CURVES_V02 [RO-RIS-MPAE-TN-091, 1/b]
RD3	Effect of Convergent Beam on Filter Transmission Curves	RO-RIS-MPAE-TN-096, D/-
RD4	In-field stray-light determination and correction	INFIELD_STRLIGHT_V03 [RO-RIS-MPAE-TN-093, 1/b]
RD5	OSIRIS Calibration Report	RO-RIS-MPAE-RP-147 D / c

2 Flat fields determination

The OSIRIS flat fields were created using the integrating sphere with the calibrated halogen lamps (near-IR and visible) and xenon lamps (mostly UV), placed at a lamp linear extension screw position of 12 mm and 50 mm. The configuration with the lamps at 12 mm is referred to as *lamps in bright position* and the one with the lamps at 50 mm as *lamps in dark position*. The intensity with the lamps in dark position is about 35 times lower than the one with the lamps in bright position.

The pre-flight flat fields are of special importance because no real flat field exposures can be obtained in flight. In fact, the internal calibration lamps do not provide homogeneous illumination (especially for the WAC) and the fields of view of the cameras are too large to obtain flat fields with celestial objects.

To create a flat field, between 3 to 5 raw images of the integrating sphere obtained with the same filter combination were used. For the NAC, the flat fields have been obtained in the delta calibration on 19-20 July 2003 and for the WAC in December 2001. Flat fields obtained in other periods (i.e. October 2001 for the WAC and in 2001 for the NAC) are not used for the calibration pipeline because the cameras were in a different configuration than the final one.

The selected images are full frame images (2048 x 2048 pixels) read out through amplifier B. Additionally all images contain 48 overclocked lines that are used to determine the bias level. All flat fields have been obtained with cold CCDs (~190 K).

Before creating the flat field, the raw images are processed: the coherent noise is removed, the bias is subtracted using the average intensity from the overclocked lines, and the overclocked lines are removed from the image. While the bad column on the WAC CCD is interpolated, dark pixels are not removed.

The flat field is created pixel by pixel. For each pixel, first the median value of the 3-5 input images is calculated. In case in one of the images the pixel value differs by more than 5σ from the median, this pixel value is rejected as being unreliable. The average of the remaining values is the value of the flat field at that pixel.

Finally, the flat fields are normalized to unity in the central 200×200 pixels region as described in Section 2.1.

The initial versions of the flat fields (V01) used by the calibration pipeline to calibrate the OSIRIS images have been created with the Disrsoft routine makeflat.pro.

2.1 Normalization of the flat field images

The flat fields are normalized to unity in the central 200×200 pixel region, dividing the image by the average value in the window [924:1123,924:1123] in CCD coordinate system.

In case of the WAC UV245 filter (F31), a pinhole is located in the center of the image. The additional intensity caused by the pinhole is corrected to calculate the normalization factor. For this image, the average over the central region is normalized to 1.0768013.

2.2 WAC flat fields

The flat fields for all WAC filter combinations are listed in Table 3. The original files (.uax) are stored in .\data\lab\FM\first_calibration\Analysis\flatfields\wac. The calibrated halogen lamps were used for the filters in the visible spectral range, while the xenon lamps were used for the UV-filters.

The lamps were operated in bright position. Halogen lamps were used for filters in the visible wavelength range, and xenon lamps were used for filters in the UV range. Only filter F12 was operated with the halogen lamp in dark position.

The initial versions of the flat fields (V01) used by the calibration pipeline to calibrate the OSIRIS images have been created with the Disrsoft routine makeflat.pro. They have been updated to remove facility artefacts as described in Section 9.

The flat fields used by the pipeline are listed in Table 5.

2.3 NAC flat fields

The flat fields for all NAC filter combinations are listed in Table 4. The original files (.uax) are stored in data\lab\FM\first_calibration\Analysis\flatfields\newnac.

Numerous filter combinations were observed with the halogen lamps, both in bright and in dark position. Two filter combinations containing the neutral density filter (F83 and F84) and combinations containing the near-UV or far-UV filters were additionally flat-fielded with the xenon lamps.

Flat fields derived from images acquired with the lamps in bright position differ up to a few percent from flat fields obtained in dark position. It was decided to use the flat fields taken with the halogen lamps in bright position as default flat fields for all filter combinations that were flat-fielded in that configuration.

The original flat field images used in the pipeline in version V01 are derived from the original .uax files by the procedure described in [RD5] and listed in Table 4. The first column contains the filenames of the flat fields called by OsiCalliope. These are equivalent to the files that were used by the IDL pipeline.

In 2015, the NAC filters affected most by these facility artefacts (F16, F24 and F84) have been corrected using in-flight calibration lamp images (see Section 2.4). After a re-evaluation in 2020, many of the NAC flat fields have been corrected by removing these facility artefacts applying a correction derived from the ratio between flats taken with lamps in bright and dark position (see Section 2.5).

2.4 Correction of calibration facility artefacts on NAC flats using in-flight calibration lamp images

Colour ratio images of the comet surface highlighted the known non uniformity of some of the NAC flat fields, in particular of the NAC F16 (Near-UV), F24 (Blue) and F84 (Blue) flat fields. Those filters are in the short wavelength part of the visible spectrum, with $\lambda_{cent} \leq 480$ nm. We will refer to the flat fields of those filters as "shorter wavelength flats" and to the flat fields of filters with $\lambda_{cent} \geq 535$ nm as "longer wavelength flats".

In the GRM delta calibration performed in 2016, the non-uniform pattern of the shorter wavelength flat fields was reproduced and attributed to illumination artefacts of the integrating sphere at the time when the images used to generate the flat fields were acquired.

Flat field images can be handled as a product of two separate images: a low spatial frequency and a high spatial frequency image.

- The high spatial frequency component shows the small scale, pixel to pixel variations. This is the effect of the CCD pixel non uniformities in size and sensitivity, and also the contamination effects on or close to the CCD surface.
- The low spatial frequency component contains the effect of the optical system, filter transmission non-uniformities, and the illumination artefacts of the target. These are large scale variations of the pixel sensitivities across the image surface.

Since the integrating sphere artefacts affect only the low spatial frequency flat fields, the correction should be applied only to this component, keeping the original high spatial frequency part unchanged.

The separation of the low and high spatial frequency components of the flat field image is done by the following procedure:

- Remove the hot and cold areas (grey level > 1.1 and grey level < 0.95) from the flat images by area patching, to avoid that they affect the averaging.
- Create the low spatial frequency image by applying a Gaussian blur filter with a size of 100 pixels.
- Normalize the low spatial frequency image to 1.00.
- Create the high spatial frequency image by dividing the original flat field by the low spatial frequency image.

The longer wavelength flats are relatively uniform, with a maximum deviation of only 2% from the average (Figure 1). The shorter wavelength flats, and especially F24, F84 and F16, show larger non-uniformity (about 5%) and a characteristic pattern near the corners (Figure 2).

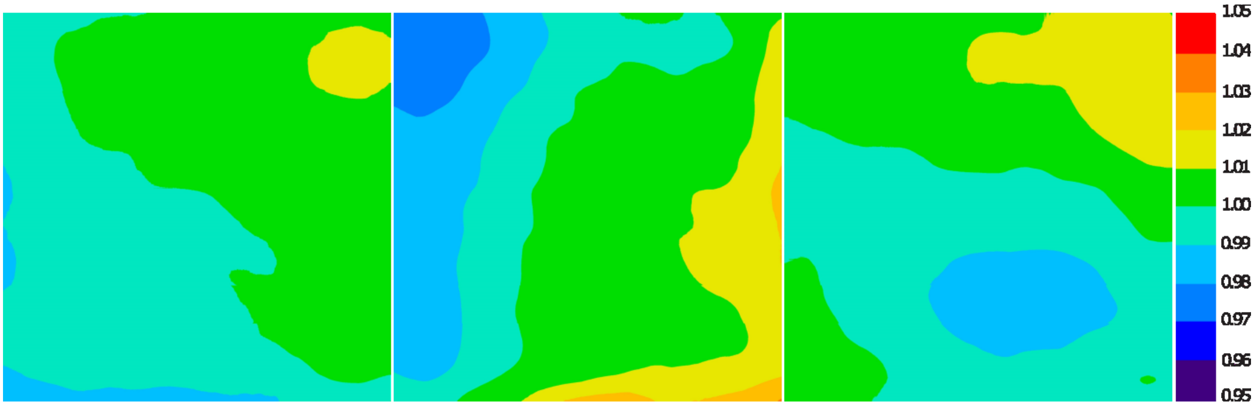

Figure 1 Original low spatial frequency flat fields for F22, F23, and F82.

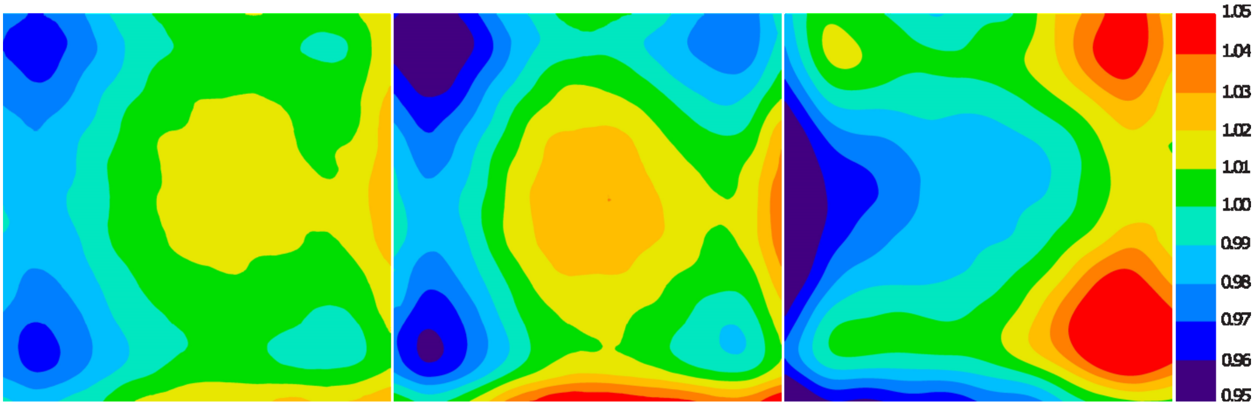

Figure 2 Original low spatial frequency flat fields for F24, F84, and F16.

Analysing the in-flight internal calibration lamp images of the NAC, the characteristic large scale non-uniformities are not visible. This indicates that these artefacts are caused by the laboratory calibration optical setup.

Consequently, if we assume that the longer wavelength flat fields are correct, the correction of the shorter wavelength flat fields can be performed using in-flight calibration lamp images:

$$FLAT_{short\_corrected} = FLAT_{long\_ref} * FLAT_{short\_lamp} / FLAT_{long\_lamp}$$

where:

$FLAT_{short\_corrected}$	the corrected shorter wavelength flat field image
$FLAT_{short\_lamp}$	the in-flight shorter wavelength calibration lamp flat field image
$FLAT_{long\_lamp}$	the in-flight longer wavelength calibration lamp flat field image
$FLAT_{long\_ref}$	the original longer wavelength reference flat field image.

For the generation of the corrected shorter wavelength flat fields we have used the flat field of the orange filter (F22) as longer wavelength reference flat field.

The generation of the new flat images is done by the following procedure:

- Generate flat field images from the calibration lamp images, for the longer wavelength and the shorter wavelength filters.
- Separate the high- and low-spatial frequency component of the original flat images, and the calibration lamp flat images.

- Calculate the corrected low spatial frequency flat image based on the above formula, using only the low spatial frequency component of the original and the calibration lamp flats.
- Generate the new flat image by multiplying the new low spatial frequency component with the original high spatial frequency component.
- Normalize the flat field to a mean of 1 in the central pixel region specified in Section 2.1 as has been done in the V01 of the flat field images.

Figure 3 shows the comparison between the original and the corrected flat fields for F16 (top row), F24 (centre row) and F84 (bottom row), respectively.

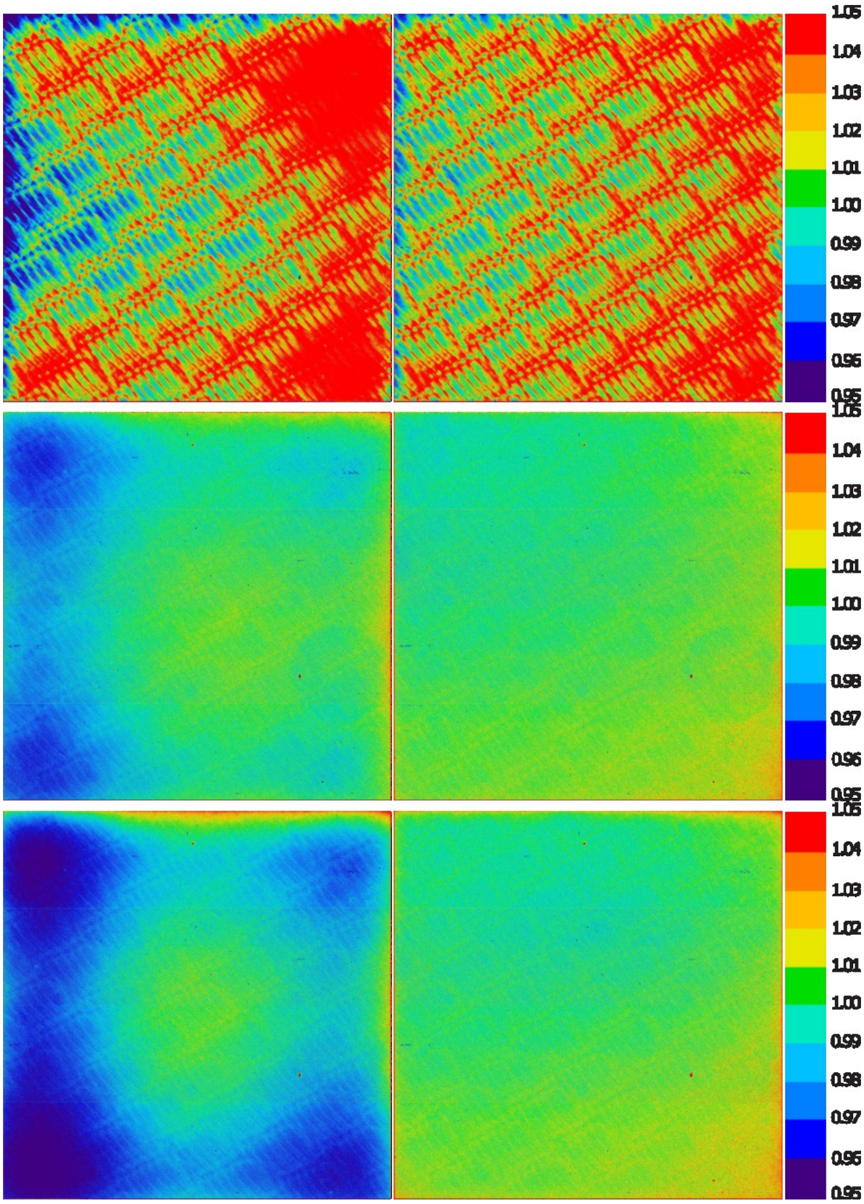

Figure 3 Original and corrected F16 (top), F24 (centre) and F84 (bottom) flat field images.

Version V02 of the flat field images for NAC filters F16, F24, and F84 on the calibration pipeline database are normalized to a mean value of 1 over the entire field, while V03 of these files are normalized only in the central part as described in Section 2.1. The flat fields currently used by the pipeline are listed in Table 5.

2.5 Correction of calibration facility artefacts on NAC flats

The versions V01 of the NAC flat images are created from the integrating sphere images of the calibration campaign 2003 July. During this sequence, several images have been acquired in different filter combinations and sphere lamp configurations. The flat field images generated with the same filter setup, but with different lamp intensity configuration exhibited a significant difference. A characteristic pattern appeared which became stronger with the illumination intensity. The main features of this pattern is equivalent to the pattern removed during correction of filters F16, F24 and F84 using the in-flight calibration lamp images. This adds further evidence that these features are indeed caused by the measurement facility and not by the optical system itself.

The ratio of high and low intensity is therefore used to correct the NAC flat field images from facility caused artefacts. In some cases, where for technical reasons (too dim for high-intensity or to right for low-intensity flat images to be acquired) no ratio can be calculated, the ratio of a filter combination close in wavelength range or sharing one of the filter plates is used for this correction.

The creation of the ratio images for NAC flats and the selection of the applicable ratio and scaling parameters is detailed in RD1.

2.5.1 Removal of facility artefacts from NAC flat field images

The normalized ratio image $I_{\mathrm{corr},ij}$ for filter Fij is used to correct the flat-field image $F_{V01,ij}$ by applying the following equation:

$$F_{\mathrm{V02},ij} = F_{\mathrm{V01},ij} \times \left(\frac{1}{1 - C_{ij}\left(I_{\mathrm{corr},ab} - 1\right)} \right)$$

Where

$F_{\mathrm{V01},ij}$	The existing flat for filter *ij*
$F_{\mathrm{V02},ij}$	The resulting flat for filter *ij*
$I_{\mathrm{corr},ab}$	The ratio calculated for filter *ab*
C_{ij}	The correction factor for filter *ij*

The correction factor C_{ij} is selected using an optimization routine to find the resulting flat $F_{\mathrm{V02},ij}$ with the smallest standard deviation of values around the mean.

The resulting flat $F_{\mathrm{V02},ij}$ is normalized to a mean of 1 in the central region specified in Section 2.1 as has been done for the versions V01 of the flat field images.

2.5.2 *Values used in the removal of facility artefacts from NAC flat field images*

Table 1 Filters corrected from facility artefacts by applying a scaled ratio image derived from a high- and a low-intensity flat field image. For details see [RD1]

NAC filter	Filter used to create ratio image	Scaling Factor	Result
15	F24	1.185515448	NAC_FM_FLAT_15_V02.IMG
22	F23	-0.254402777	NAC_FM_FLAT_22_V02.IMG
23	F23	0.908609654	NAC_FM_FLAT_23_V02.IMG
27	F27	-1.449450308	NAC_FM_FLAT_27_V02.IMG
32	F23	-0.27670016	NAC_FM_FLAT_32_V02.IMG
33	F33	0.953520483	NAC_FM_FLAT_33_V02.IMG
34	F34	1.285422361	NAC_FM_FLAT_34_V02.IMG
37	F37	-1.740223919	NAC_FM_FLAT_37_V02.IMG
51	F51	0.249548661	NAC_FM_FLAT_51_V02.IMG
58	F58	-3.105952621	NAC_FM_FLAT_58_V02.IMG
61	F61	-3.028675205	NAC_FM_FLAT_61_V02.IMG
71	F71	-4.013424754	NAC_FM_FLAT_71_V02.IMG
82	F82	-2.015544792	NAC_FM_FLAT_82_V02.IMG
83	F23	2.105817467	NAC_FM_FLAT_83_V02.IMG
87	F87	-1.631721012	NAC_FM_FLAT_87_V02.IMG
88	F88	-0.627891765	NAC_FM_FLAT_88_V02.IMG

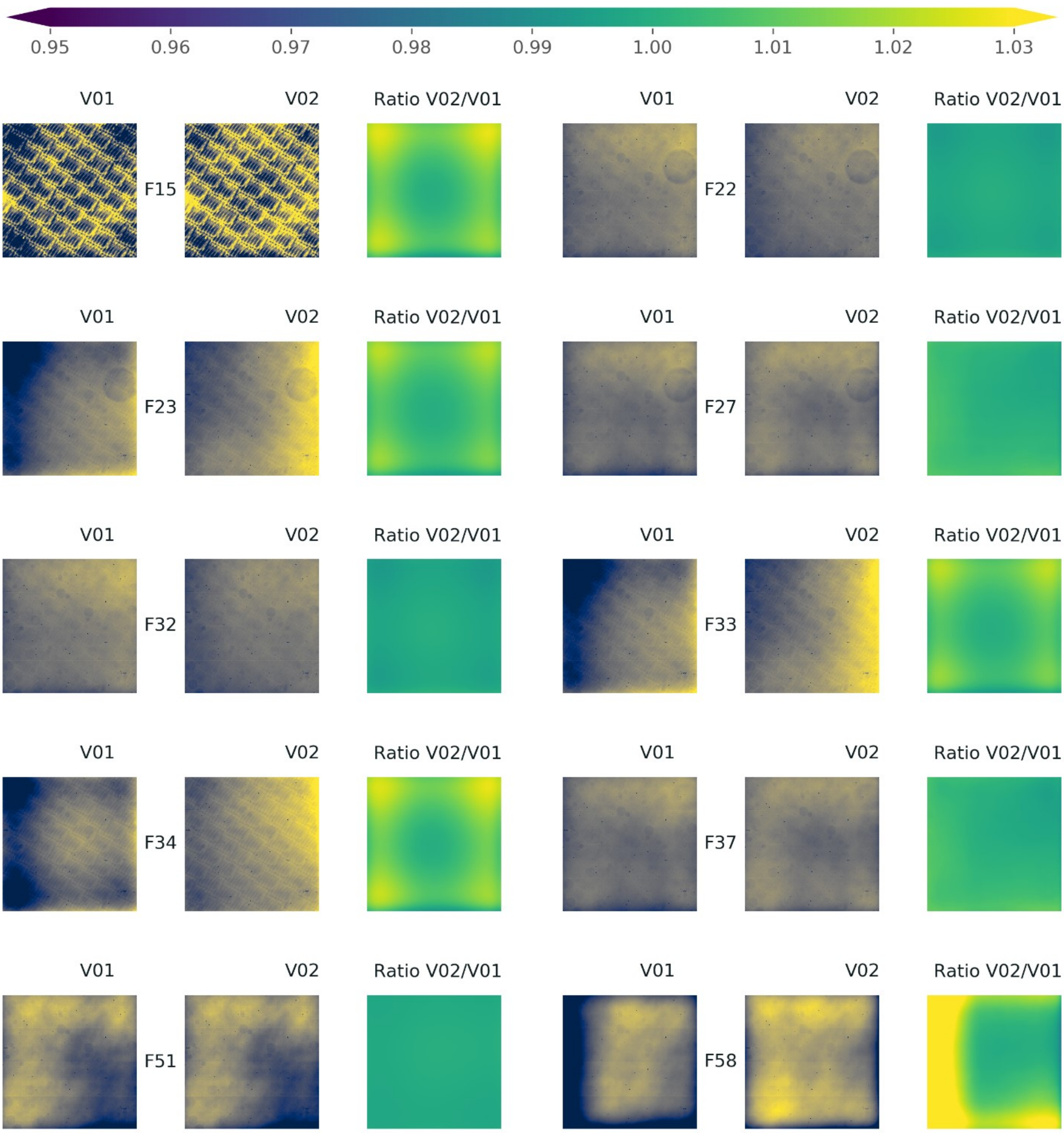

Figure 4 NAC flat field files corrected for facility artefacts using ratios of high-to low-intensity flat field images. The colour scale is calculated for individual pairs of V01 and V02 of the same filter, but all ratio images are scaled based on the colour bar on the top of the image.

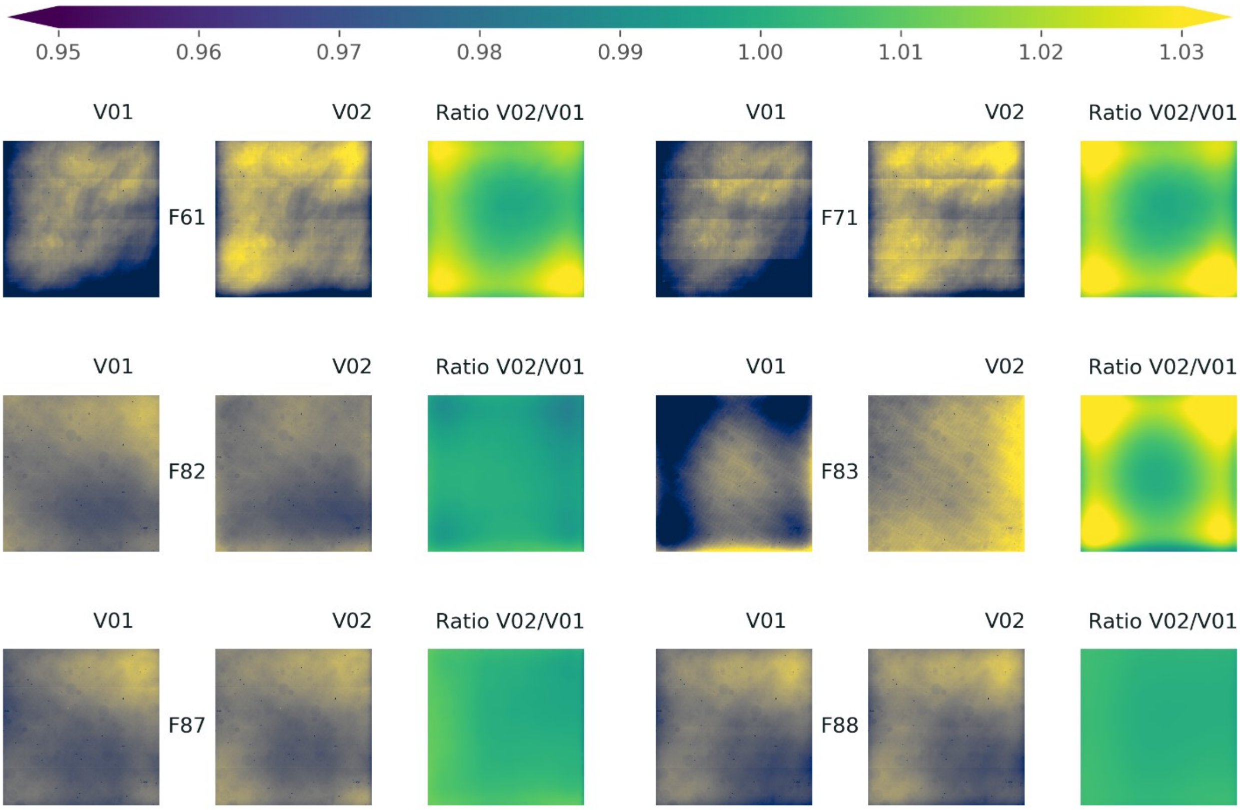

Figure 4 continued.

2.6 Correction of calibration facility artefacts on WAC flats

The features in the calibration facility causing the artefacts seen in NAC flat fields are also manifest in WAC flat field files of the original flat fielding campaign, even though by the different focal length and optical properties appearing in different shapes and sizes. The artefacts are defocused, dark areas with circular and elliptical shape, and present on all filter images. They showed significant displacements between calibration campaigns in 2001 October and December, as seen in Figure 5. This is attributed to the horizontal position variation of the integrating sphere position or a different camera alignment between the two measurements, which is a strong indication for a non-camera, thus facility, nature.

The WAC focal length is relatively short, so the marked spots on the flat images are likely due to the sphere back surface non-uniformity, and the different reflection of the flattened back section.

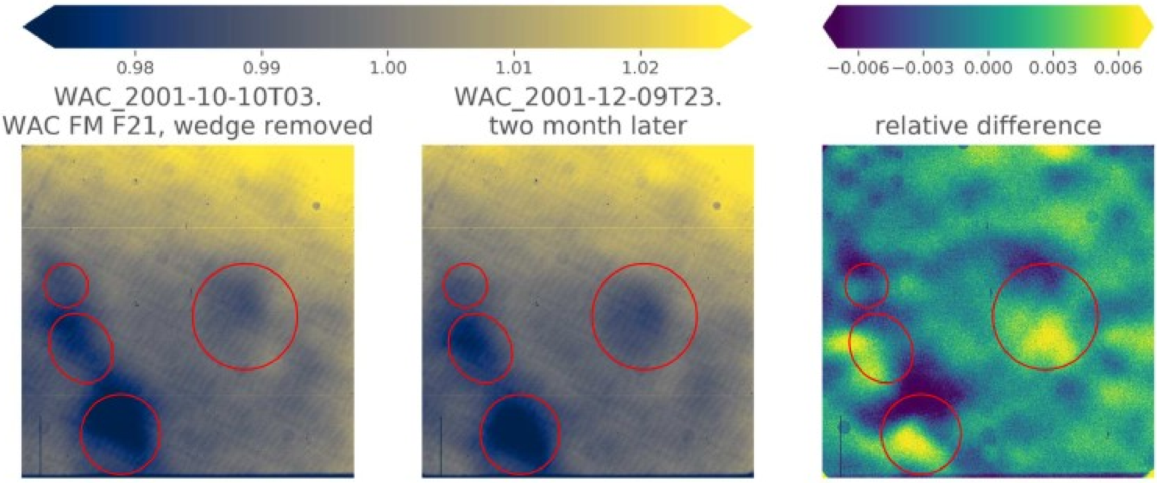

Figure 5 Two images of the WAC F21 taken during the flat field campaign two month apart. For display purposes, the first-order gradient caused by the off-axis optical system is removed and the images are normalized. The marked regions contain features that move in location. The images are WAC_2001-10-10T 03.23.55.061Z_ID00_0000008827_F21.uax (left) and WAC_2001-12-9T23.15.21.300Z_ID00_00000 10015_F21.uax (centre). The relative difference is calculated by $\boldsymbol{\Delta_{\mathrm{rel}}} = \mathbf{2} \cdot (\boldsymbol{I_{\mathrm{left}}} - \boldsymbol{I_{\mathrm{right}}})/(\boldsymbol{I_{\mathrm{left}}} + \boldsymbol{I_{\mathrm{right}}})$

To correct the above effect, synthetic correction images were generated based on the same method as the ghost patterns in case of the in-field stray light removal [RD4]. Each pattern is defined as a disk centred at position X, Y with a radius of R_p. This disk is scaled to intensity A and a Gaussian blur of width G is applied .An exemplary synthetic artefact created with the parameters in Table 2 is shown in Figure 6.

Table 2 Parameters of the synthetic artefact shown in Figure 6. For a detailed explanation, see [RD4]. . The Gaussian blur parameter is chosen as $\boldsymbol{G}$ = 400px.

Pattern	Centre $\boldsymbol{X}$	Centre $\boldsymbol{Y}$	Radius $\boldsymbol{R_p}$	Intensity $\boldsymbol{A}$
1	1312	1012	130	-0.003
2	1312	1012	200	-0.02
3	586	1736	130	-0.04
4	228	1180	130	-0.03
5	328	1380	120	-0.03
6	200	900	80	-0.04

Figure 6 Exemplary synthetic artefact created by the ghost pattern above using the method described in [RD4]. These patterns are optimized to eliminate the facility artefacts seen in Figure 5.

The pattern components are individually tuneable. For each WAC filter combination the synthetic artefact image is optimized and reviewed to eliminate the features seen in Figure 5. The result is shown in Figure 7.

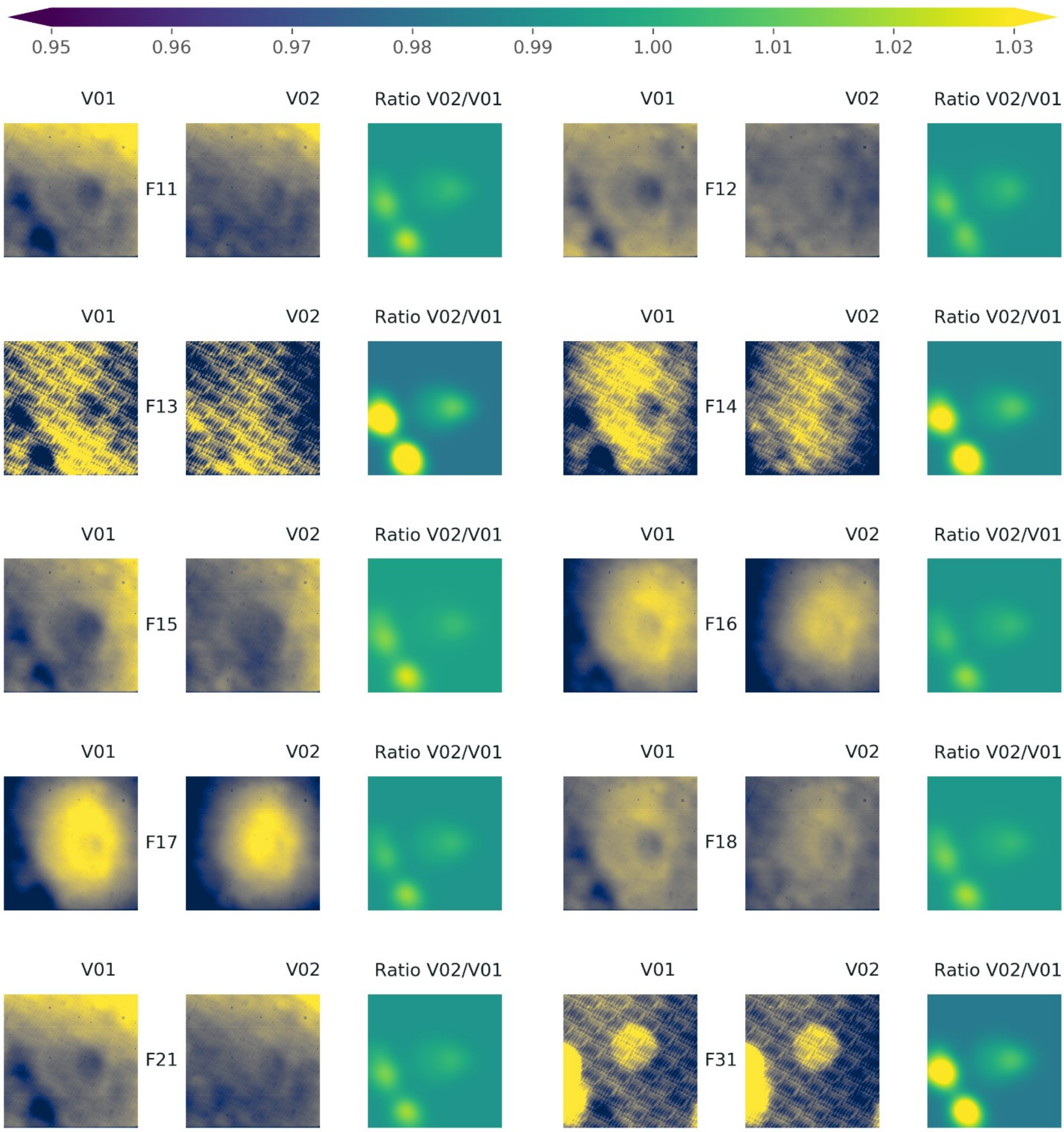

Figure 7 WAC Flat field files corrected for facility artefacts. For display purposes, the gradient caused by the off-axis optical system is removed. The colour scale is calculated for individual pairs of V01 and V02 of the same filter, but all ratio images are scaled based on the colour bar on the top of the image.

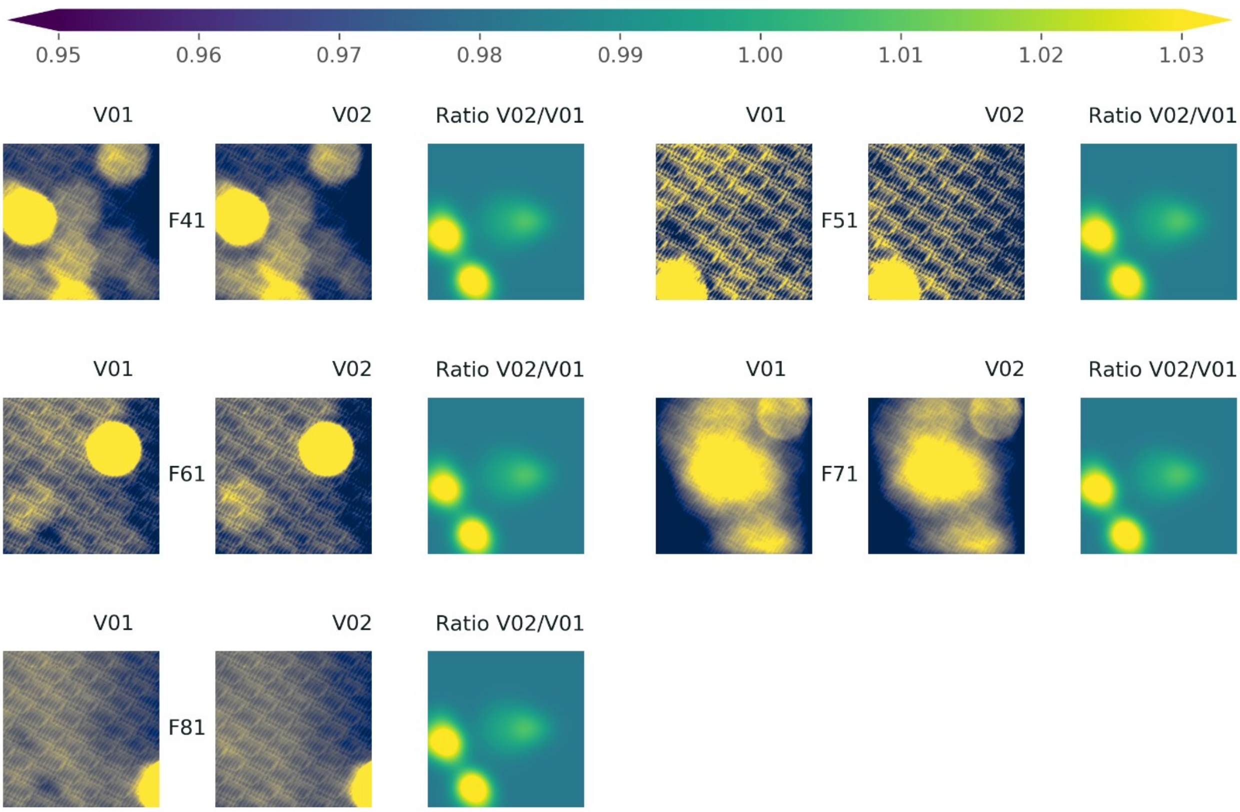

Figure 7 continued. The colour bar on the top of the image and is the same as in Figure 7.

2.7 Synthetic flat field images

For the WAC filter F11, as well as the NAC filter F31 and the NAC filter F81 no laboratory measurements are available.

The flat field of the WAC F11 filter has been synthetically generated as weighted average of existing visible wavelength flat fields. As weighting factor we have used the CCD quantum efficiency at the central wavelength of each filter.

The NAC F31 flat field image NAC_FM_FLAT_31_V01.IMG is the pixel-wise average of the following files: NAC_FM_FLAT_32_V02.IMG, NAC_FM_FLAT_38_V01.IMG, NAC_FM_FLAT_21_V01.IMG.

The NAC F81 flat field image NAC_FM_FLAT_81_V01.IMG is the pixel-wise average of the following files: NAC_FM_FLAT_82_V02.IMG, NAC_FM_FLAT_87_V02.IMG, NAC_FM_FLAT_88_V02.IMG.

3 Spectral Correction

The flat field images acquired with the integrating sphere in 2001 and 2003 were illuminated with either halogen or xenon lamps (the light source per filter is specified in Table 3 and Table 4), with a known spectral characteristic $E_{\text{sphere}}(\lambda)$ of the resulting flux including sphere coating. Observed solar system objects reflect solar light and thus show in first approximation the spectral characteristic of the Sun E_{Sun}.

It is moreover known from measurements of flight spare filters in 2012 that the filter transmission curve changes as a function of the incidence angle of the beam. The transmission curve shifts to smaller wavelengths for increasing angles of incidence and also changes its shape and integral [RD2]. As the incidence angle of the principle rays varies from 6.7 to 11.5 degrees within the field of the WAC, also the transmission curve changes as a function of this angle. For the NAC, this variation is from 4.30 to 4.37 degree such that the transmission variation is negligible.

As a consequence, a flat field image acquired with a halogen or xenon source would be different when acquired with a solar source spectrum. The difference for each pixel is the ratio of the integrated flux from a solar spectrum divided by the sphere spectrum $R_{\mathrm{Sun}}/R_{\mathrm{sphere}}$, where

$$R_{\mathrm{source}} = \int E_{\mathrm{source}}(\lambda) \cdot S(\lambda, \theta)\, d\lambda$$

is the integrated spectral flux of a source, with source being either Sun or sphere. The instrument sensitivity S depends on the wavelength λ and on the angle of incidence θ of the principle ray of a given pixel. Note that the actual flux per pixel comes from a distribution of incidence angles due to the convergence of the beam in the optical system. But the principle ray (or chief ray) is used as a good approximation for the effective angle [RD3].

The ratio $R_{\mathrm{Sun}}/R_{\mathrm{sphere}}$ was calculated for each filter and each pixel and normalised to the central 200×200 pixels (also see 2.1). Typical ranges of these correction images are $\pm 1\%$ with respect to the centre between left and right, where CN filter shows the largest variation of $\pm 2.2\%$. In the calibration pipeline, the image is divided by this *spectral correction flat field* immediately after the laboratory flat field correction.

OSIRIS images are thus flattened for a solar type spectrum.

For the analysis of objects with other spectra, the image needs to be converted by multiplying an OSIRIS Level 2 (CODMAC L3) image with the solar spectral correction and divided by the spectral correction of the target of choice. The two spectral correction images that are provided with the OSIRIS data sets are $R_{\mathrm{Sun}}/R_{\mathrm{lamp}}$ and $R_{\mathrm{Vega}}/R_{\mathrm{lamp}}$, which are stored as layers SUN_IMAGE and VEGA_IMAGE in files with the name WAC_FM_SPEC_ij_V01.IMG, where ij is the filter combination.

The correction is not required for WAC filter 11 (empty) as there is no filter shift without filter.

4 Error estimation of flat-field images

During the removal of facility artefacts the strongest artefacts found in the images have been removed. This resulted in a change of up to 2% of the flat field images. It is therefore reasonable to assume that no facility artefact feature above the 1% level remains in the flat field image. We therefore estimate the absolute error of the flat field to $\sigma_{F_{\mathrm{lab}}} = 0.01$.

In the flat-fielding, the corrected image $\overline{\boldsymbol{N}}_{\mathrm{labflat}}$ is calculated from the bias corrected image $\overline{\boldsymbol{N}}_{\mathrm{bias}}$ using the laboratory flat field $\overline{\boldsymbol{F}}_{\mathrm{lab}}$

$$\overline{\boldsymbol{N}}_{\mathrm{labflat}} = \frac{\overline{\boldsymbol{N}}_{\mathrm{bias}}}{\overline{\boldsymbol{F}}_{\mathrm{lab}}}$$

Therefore the error contribution of the flat fielding step to the total error map is estimated as

$$\sigma_{\overline{\boldsymbol{N}}_{\mathrm{labflat}}} = \overline{\boldsymbol{N}}_{\mathrm{labflat}} \cdot \sqrt{\left(\frac{\sigma_{\overline{\boldsymbol{N}}_{\mathrm{bias}}}}{\overline{\boldsymbol{N}}_{\mathrm{bias}}}\right)^2 + \left(\frac{\boldsymbol{\sigma}_{\boldsymbol{F}_{\mathbf{lab}}}}{\overline{\boldsymbol{F}}_{\mathrm{lab}}}\right)^2}$$

where

$\sigma_{\overline{\boldsymbol{N}}_{\mathrm{labflat}}}$	Is the error map after the flat-fielding step.
$\overline{\boldsymbol{N}}_{\mathrm{labflat}}$	Is the image after the flat-fielding step
$\overline{\boldsymbol{N}}_{\mathrm{bias}}$	Is the image after the bias correction step, that is the step before the flat-field correction in the calibration pipeline
$\sigma_{\overline{\boldsymbol{N}}_{\mathrm{bias}}}$	Is the error map after the bias correction step
$\overline{\boldsymbol{F}}_{\mathrm{lab}}$	Is the laboratory flat field image used
$\boldsymbol{\sigma}_{\boldsymbol{F}_{\mathbf{lab}}}$	Is the relative level of imperfections remaining in the laboratory flat field images. $\sigma_{F_{\mathrm{lab}}} = 0.01$

5 List of flat fields from ground calibration

Table 3 List of WAC flat fields.

Filename[a]	Original filename[b]	Old filename[c]	Image IDs[d]	T [s][e]	Filters[f]	Lamps[g]	Position[h]
WAC_FM_FLAT_16_V01.IMG	flat_wac_empty1_na_h_12.uax	WAC_FM_FLAT-16_V1_28062005.img	10670-10674	0.20	F16	Halogen	bright
WAC_FM_FLAT_17_V01.IMG	flat_wac_empty1_oi_h_12.uax	WAC_FM_FLAT-17_V1_28062005.img	10675-10679	0.25	F17	Halogen	bright
WAC_FM_FLAT_18_V01.IMG	flat_wac_empty1_vis610_h_12.uax	WAC_FM_FLAT-18_V1_28062005.img	10681-10685	0.07	F18	Halogen	bright
WAC_FM_FLAT_15_V01.IMG	flat_wac_empty1_nh2_h_12.uax	WAC_FM_FLAT-15_V1_28062005.img	10687,10688, 10690-10692	0.12	F15	Halogen	bright
WAC_FM_FLAT_21_V01.IMG	flat_wac_green_empty2_h_12.uax	WAC_FM_FLAT-21_V1_28062005.img	10696-10700	0.03	F21	Halogen	bright
WAC_FM_FLAT_12_V01.IMG	flat_wac_empty1_r_h_50.uax	WAC_FM_FLAT-12_V1_28062005.img	10738,10741-10743,10746	0.12	F12	Halogen	dark
WAC_FM_FLAT_31_V01.IMG	flat_wac_uv245_empty2_x_12.uax	WAC_FM_FLAT-31_V1_28062005.img	10806-10810	6.00	F31	Xenon	bright
WAC_FM_FLAT_41_V01.IMG	flat_wac_cs_empty2_x_12.uax	WAC_FM_FLAT-41_V1_28062005.img	10815-10819	12.00	F41	Xenon	bright
WAC_FM_FLAT_51_V01.IMG	flat_wac_uv295_empty2_x_12.uax	WAC_FM_FLAT-51_V1_28062005.img	10825-10829	6.00	F51	Xenon	bright
WAC_FM_FLAT_61_V01.IMG	flat_wac_oh308_empty2_x_12.uax	WAC_FM_FLAT-61_V1_28062005.img	10834-10838	6.00	F61	Xenon	bright
WAC_FM_FLAT_71_V01.IMG	flat_wac_uv325_empty2_x_12.uax	WAC_FM_FLAT-71_V1_28062005.img	10842,10843, 10845-10847	1.00	F71	Xenon	bright
WAC_FM_FLAT_81_V01.IMG	flat_wac_nh335_empty2_x_12.uax	WAC_FM_FLAT-81_V1_28062005.img	10852-10855	3.00	F81	Xenon	bright
WAC_FM_FLAT_13_V01.IMG	flat_wac_empty1_uv375_x_12.uax	WAC_FM_FLAT-13_V1_28062005.img	10862-10866	0.45	F13	Xenon	bright
WAC_FM_FLAT_14_V01.IMG	flat_wac_empty1_cn_x_12.uax	WAC_FM_FLAT-14_V1_28062005.img	10873-10877	0.50	F14	Xenon	bright

[a]: file name as in the OsiCalliope database. [b]: file name of the original flat field images in uax format. [c]: filename used to store the flat fields images in the IDL pipeline database. [d]: IDs of the images that were used to create the flat field (taken from the list obtained by the IDL procedure readfilelist, corresponding to the index in the file .\osiris\IDL\disrsoft\cal_soft\osirsoft\database\ filelists\filelist.out on CVS). [e]: exposure time. [f]: the filter positions. [g] and [h]: lamps and their positions.

Table 4 List of NAC flat fields.

Filename[a]	Original filename[b]	Old filename[c]	Image IDs[d]	T [s][e]	Filters[f]	Lamps[g]	Position[h]
NAC_FM_FLAT_82_V01.IMG	flat_nac_neutral_orange_h_50.uax	NAC_FM_FLAT-82_V1_28062005.img	14677-14681	16.000	F82	Halogen	dark
	flat_nac_neutral_green_h_50.uax		14689-14693	50.000	F83	Halogen	dark
	flat_nac_neutral_blue_h_50.uax		14705-14709	75.000	F84	Halogen	dark
NAC_FM_FLAT_87_V01.IMG	flat_nac_neutral_hydra_h_50.uax	NAC_FM_FLAT-87_V1_28062005.img	14719-14723	20.000	F87	Halogen	dark
NAC_FM_FLAT_88_V01.IMG	flat_nac_neutral_red_h_50.uax	NAC_FM_FLAT-88_V1_28062005.img	14734-14738	8.000	F88	Halogen	dark
NAC_FM_FLAT_22_V01.IMG	flat_nac_ffp-vis_orange_h_50.uax	NAC_FM_FLAT-22_V1_28062005.img	14753-14757	0.800	F22	Halogen	dark
NAC_FM_FLAT_23_V01.IMG	flat_nac_ffp-vis_green_h_50.uax	NAC_FM_FLAT-23_V1_28062005.img	14764-14768	3.000	F23	Halogen	dark
NAC_FM_FLAT_24_V01.IMG	flat_nac_ffp-vis_blue_h_50.uax	NAC_FM_FLAT-24_V1_28062005.img	14778-14782	5.000	F24	Halogen	dark
NAC_FM_FLAT_27_V01.IMG	flat_nac_ffp-vis_hydra_h_50.uax	NAC_FM_FLAT-27_V1_28062005.img	14795-14799	1.000	F27	Halogen	dark
NAC_FM_FLAT_28_V01.IMG	flat_nac_ffp-vis_red_h_50.uax	NAC_FM_FLAT-28_V1_28062005.img	14809-14813	0.400	F28	Halogen	dark
NAC_FM_FLAT_32_V01.IMG	flat_nac_nfp-vis_orange_h_50.uax	NAC_FM_FLAT-32_V1_28062005.img	14823-14827	0.800	F32	Halogen	dark
NAC_FM_FLAT_33_V01.IMG	flat_nac_nfp-vis_green_h_50.uax	NAC_FM_FLAT-33_V1_28062005.img	14843-14847	3.000	F33	Halogen	dark
NAC_FM_FLAT_34_V01.IMG	flat_nac_nfp-vis_blue_h_50.uax	NAC_FM_FLAT-34_V1_28062005.img	14861-14865	5.000	F34	Halogen	dark
NAC_FM_FLAT_37_V01.IMG	flat_nac_nfp-vis_hydra_h_50.uax	NAC_FM_FLAT-37_V1_28062005.img	14873-14877	1.000	F37	Halogen	dark
NAC_FM_FLAT_38_V01.IMG	flat_nac_nfp-vis_red_h_50.uax	NAC_FM_FLAT-38_V1_28062005.img	14894-14898	0.400	F38	Halogen	dark
NAC_FM_FLAT_51_V01.IMG	flat_nac_ortho_ffp-ir_h_50.uax	NAC_FM_FLAT-51_V1_28062005.img	14904-14908	2.000	F51	Halogen	dark
NAC_FM_FLAT_58_V01.IMG	flat_nac_ortho_red_h_50.uax	NAC_FM_FLAT-58_V1_28062005.img	14918-14922	20.000	F58	Halogen	dark
NAC_FM_FLAT_41_V01.IMG	flat_nac_nir_ffp-ir_h_50.uax	NAC_FM_FLAT-41_V1_28062005.img	14936-14940	1.500	F41	Halogen	dark

Filename[a]	Original filename[b]	Old filename[c]	Image IDs[d]	T [s][e]	Filters[f]	Lamps[g]	Position[h]
NAC_FM_FLAT_61_V01.IMG	flat_nac_fe2o3_ffp-ir_h_50.uax	NAC_FM_FLAT-61_V1_28062005.img	14950-14954	3.000	F61	Halogen	dark
NAC_FM_FLAT_71_V01.IMG	flat_nac_ir990_ffp-ir_h_50.uax	NAC_FM_FLAT-71_V1_28062005.img	14964-14968	6.000	F71	Halogen	dark
NAC_FM_FLAT_21_V01.IMG	flat_nac_ffp-vis_ffp-ir_h_50.uax	NAC_FM_FLAT-21_V1_28062005.img	14979-14983	0.100	F21	Halogen	dark
	flat_nac_neutral_orange_h_12.uax		15064-15068	0.800	F82	Halogen	bright
NAC_FM_FLAT_83_V01.IMG	flat_nac_neutral_green_x_12.uax	NAC_FM_FLAT-83_V1_28062005.img	15071-15075	3.333	F83	Xenon	bright
NAC_FM_FLAT_84_V01.IMG	flat_nac_neutral_blue_x_12.uax	NAC_FM_FLAT-84_V1_28062005.img	15078-15082	6.666	F84	Xenon	bright
	flat_nac_neutral_hydra_h_12.uax		15085-15089	1.666	F87	Halogen	bright
	flat_nac_neutral_red_h_12.uax		15092-15096	0.500	F88	Halogen	bright
	flat_nac_ffp-vis_green_h_12.uax		15099-15103	0.100	F23	Halogen	bright
	flat_nac_ffp-vis_blue_h_12.uax		15106-15110	0.166	F24	Halogen	bright
	flat_nac_ffp-vis_hydra_h_12.uax		15113-15117	0.083	F27	Halogen	bright
	flat_nac_nfp-vis_green_h_12.uax		15120-15124	0.100	F33	Halogen	bright
	flat_nac_nfp-vis_blue_h_12.uax		15127-15131	0.166	F34	Halogen	bright
	flat_nac_nfp-vis_hydra_h_12.uax		15134-15138	0.066	F37	Halogen	bright
	flat_nac_ortho_ffp-ir_h_12.uax		15141-15145	0.066	F51	Halogen	bright
	flat_nac_ortho_red_h_12.uax		15148-15152	0.666	F58	Halogen	bright
	flat_nac_nir_ffp-ir_h_12.uax		15155-15159	0.050	F41	Halogen	bright
	flat_nac_fe2o3_ffp-ir_h_12.uax		15162-15166	0.100	F61	Halogen	bright

Filename[a]	Original filename[b]	Old filename[c]	Image IDs[d]	T [s][e]	Filters[f]	Lamps[g]	Position[h]
	flat_nac_ir990_ffp-ir_h_12.uax		15169-15173	0.200	F71	Halogen	bright
NAC_FM_FLAT_15_V01.IMG	flat_nac_ffp-uv_fuv_x_12.uax	NAC_FM_FLAT-15_V1_28062005.img	15189-15193	3.500	F15	Xenon	bright
NAC_FM_FLAT_16_V01.IMG	flat_nac_ffp-uv_nuv_x_12.uax	NAC_FM_FLAT-16_V1_28062005.img	15207-15211	0.100	F16	Xenon	bright
	flat_nac_neutral_blue_x_12.uax		15223-15227	0.500	F84	Xenon	bright
	flat_nac_neutral_green_x_12.uax		15240-15244	0.700	F83	Xenon	bright
NAC_FM_FLAT_26_V01.IMG	flat_nac_ffp-vis_nuv_x_12.uax	NAC_FM_FLAT-26_V1_28062005.img	15257-15261	0.150	F26	Xenon	bright
NAC_FM_FLAT_36_V01.IMG	flat_nac_nfp-vis_nuv_x_12.uax	NAC_FM_FLAT-36_V1_28062005.img	15275-15279	0.150	F36	Xenon	bright
NAC_FM_FLAT_35_V01.IMG	flat_nac_nfp-vis_fuv_x_12.uax	NAC_FM_FLAT-35_V1_28062005.img	15292-15296	12.000	F35	Xenon	bright
NAC_FM_FLAT_86_V01.IMG	flat_nac_neutral_nuv_x_12.uax	NAC_FM_FLAT-86_V1_28062005.img	15309-15313	30.000	F86	Xenon	bright

[a]: file name as in the OsiCalliope database. [b]: file name of the original flat field images in uax format. [c]: filename used to store the flat fields images in the IDL pipeline database. [d]: IDs of the images that were used to create the flat (taken from the list obtained by the IDL procedure readfilelist, corresponding to the index in the file .\osiris\IDL\disrsoft\cal_soft\osirsoft\database\ filelists\filelist.out on CVS). . [e]: exposure time. [f]: the filter positions. [g] and [h]: lamps and their positions.

6 Calibration files used by OsiCalliope

The calibration files used by OsiCalliope to calibrate OSIRIS images are listed in Table 5 and Table 6.

Table 5 List of the NAC and WAC flat fields used by OsiCalliope

NAC		WAC	
Filter	**Flat field filename**	**Filter**	**Flat field filename**
F15	NAC_FM_FLAT_15_V02.IMG	F11	WAC_FM_FLAT_11_V02.IMG
F16	NAC_FM_FLAT-16_V03.IMG	F12	WAC_FM_FLAT_12_V02.IMG
F22	NAC_FM_FLAT_22_V02.IMG	F13	WAC_FM_FLAT_13_V02.IMG
F23	NAC_FM_FLAT_23_V02.IMG	F14	WAC_FM_FLAT_14_V02.IMG
F24	NAC_FM_FLAT_24_V03.IMG	F15	WAC_FM_FLAT_15_V02.IMG
F27	NAC_FM_FLAT_27_V02.IMG	F16	WAC_FM_FLAT_16_V02.IMG
F28	NAC_FM_FLAT_28_V01.IMG	F17	WAC_FM_FLAT_17_V02.IMG
F31	NAC_FM_FLAT_31_V01.IMG	F18	WAC_FM_FLAT_18_V02.IMG
F32	NAC_FM_FLAT_32_V02.IMG	F21	WAC_FM_FLAT_21_V02.IMG
F33	NAC_FM_FLAT_33_V02.IMG	F31	WAC_FM_FLAT_31_V02.IMG
F34	NAC_FM_FLAT_34_V02.IMG	F41	WAC_FM_FLAT_41_V02.IMG
F37	NAC_FM_FLAT_32_V01.IMG	F51	WAC_FM_FLAT_51_V02.IMG
F38	NAC_FM_FLAT_38_V01.IMG	F61	WAC_FM_FLAT_61_V02.IMG
F81	NAC_FM_FLAT_81_V01.IMG	F71	WAC_FM_FLAT_71_V02.IMG
F82	NAC_FM_FLAT_82_V02.IMG	F81	WAC_FM_FLAT_81_V02.IMG
F83	NAC_FM_FLAT_83_V02.IMG		
F84	NAC_FM_FLAT_84_V03.IMG		
F87	NAC_FM_FLAT_87_V02.IMG		
F88	NAC_FM_FLAT_88_V02.IMG		
F41	NAC_FM_FLAT_41_V01.IMG		
F51	NAC_FM_FLAT_51_V02.IMG		
F61	NAC_FM_FLAT_61_V02.IMG		
F71	NAC_FM_FLAT_71_V02.IMG		
F58	NAC_FM_FLAT_58_V02.IMG		
F21	NAC_FM_FLAT_21_V01.IMG		
F26	NAC_FM_FLAT_26_V01.IMG		
F36	NAC_FM_FLAT_36_V01.IMG		
F35	NAC_FM_FLAT_35_V01.IMG		
F86	NAC_FM_FLAT_86_V01.IMG		

Table 6 List of spectral flat fields.

Filter	Filename
12	WAC_FM_SPEC_12_V01.IMG
13	WAC_FM_SPEC_13_V01.IMG
14	WAC_FM_SPEC_14_V01.IMG
15	WAC_FM_SPEC_15_V01.IMG
16	WAC_FM_SPEC_16_V01.IMG
17	WAC_FM_SPEC_17_V01.IMG
18	WAC_FM_SPEC_18_V01.IMG
21	WAC_FM_SPEC_21_V01.IMG
31	WAC_FM_SPEC_31_V01.IMG
41	WAC_FM_SPEC_41_V01.IMG
51	WAC_FM_SPEC_51_V01.IMG
61	WAC_FM_SPEC_61_V01.IMG
71	WAC_FM_SPEC_71_V01.IMG
81	WAC_FM_SPEC_81_V01.IMG

6.1 Previous versions

Table 7 lists previous versions of NAC and WAC flat fields in the deprecated naming convention of early versions of the calibration pipeline. Those files are obsolete, but they are identical to the files listed in Table 5 in versions V01 (V02 for filters NAC F16, F24 and F84).

Table 7 List of the previous versions of NAC and WAC flat fields.

NAC		WAC	
Filter	**Flat field filename**	**Filter**	**Flat field filename**
F15	NAC_FM_FLAT-15.img	F11	WAC_FM_FLAT-11.img
F16	NAC_FM_FLAT-16_v02.img	F12	WAC_FM_FLAT-12.img
F22	NAC_FM_FLAT-22.img	F13	WAC_FM_FLAT-13.img
F23	NAC_FM_FLAT-23.img	F14	WAC_FM_FLAT-14.img
F24	NAC_FM_FLAT-24_v02.img	F15	WAC_FM_FLAT-15.img
F27	NAC_FM_FLAT-27.img	F16	WAC_FM_FLAT-16.img
F28	NAC_FM_FLAT-28.img	F17	WAC_FM_FLAT-17.img
F32	NAC_FM_FLAT-32.img	F18	WAC_FM_FLAT-18.img
F33	NAC_FM_FLAT-33.img	F21	WAC_FM_FLAT-21.img
F34	NAC_FM_FLAT-34.img	F31	WAC_FM_FLAT-31.img
F37	NAC_FM_FLAT-37.img	F41	WAC_FM_FLAT-41.img
F38	NAC_FM_FLAT-38.img	F51	WAC_FM_FLAT-51.img
F82	NAC_FM_FLAT-82.img	F61	WAC_FM_FLAT-61.img
F83	NAC_FM_FLAT-83.img	F71	WAC_FM_FLAT-71.img
F84	NAC_FM_FLAT-84_v02.img	F81	WAC_FM_FLAT-81.img
F87	NAC_FM_FLAT-87.img		
F88	NAC_FM_FLAT-88.img		
F41	NAC_FM_FLAT-41.img		
F51	NAC_FM_FLAT-51.img		
F61	NAC_FM_FLAT-61.img		
F71	NAC_FM_FLAT-71.img		
F58	NAC_FM_FLAT-58.img		
F21	NAC_FM_FLAT-21.img		
F26	NAC_FM_FLAT-26.img		
F36	NAC_FM_FLAT-36.img		
F35	NAC_FM_FLAT-35.img		
F86	NAC_FM_FLAT-86.img		